Early Detection of Bark Beetle Induced Forest Stress using Sentinel-2 Data

LISA MANDL[1,2] & STEFAN LANG[2]

Abstract: Abiotic as well as biotic disturbances are central shapers of forest ecosystems. In contrast to sudden disturbance agents such as wind, avalanches and fire, bark beetle infestation is characterized by successive progression. When infestation is observable by the human eye, trees are already in the final stages of infestation - the so-called red- and grey-attack. In the relevant phase - the green-attack - biochemical and biophysical processes take place, which, however, are not or hardly visible. In this study, we applied a time series analysis based on semantically enriched Sentinel-2 data and spectral vegetation indices (SVI's) to detect early traces of bark beetle infestation in the Berchtesgaden National Park. Results show that the best separability of healthy and early-infested pixels is in the vegetation red-edge and SWIR parts of the electromagnetic spectrum. Regarding the indices, water stress-related ones have proven to be most sensitive. This method detects initial bark beetle infestation up to three weeks before sightings in the field. From a site-specific perspective, bark beetle areas are reflected with an accuracy of 76% compared to reference data.

1 Introduction

Whilst access to environmental data grew rapidly in the last decade, constant monitoring for a full understanding of forest disturbance mechanisms is still a big challenge. The launch of the Sentinel-2 satellites within the European Copernicus programme has made a major contribution to the monitoring of ecological and forestry issues and marked a paradigm shift in Earth observation (EO) monitoring capabilities (FER et al. 2021). The ultimate goal of space assets such as EO is to convert these "big Earth data" to valuable information in order to contribute to the understanding of - inter alia - natural processes (SUDMANNS et al. 2020). When it comes to the monitoring of early stress factors for vegetation, the temporal availability of satellite data is of particular importance. In this study, we developed a method to detect early infestation stages of the European Spruce Bark Beetle (*Ips typographus L.*) using semantically enriched Sentinel-2 time series and spectral vegetation indices (SVI's). Bark beetle infestation impacts forest ecosystem dynamics and consequently affect ecosystem services. Although insect disturbances lead to disrupted structures and alter the composition of the ecosystem, they also foster diversity on the landscape and thus contribute to a various number of ecosystem services (THOM & SEIDL 2016). Regardless whether considering such disturbances an opportunity or a risk, installing a monitoring system is key to gain knowledge about the ecological processes or to limit the ecological damage caused by bark beetle infestations. Both scenarios depend on the management strategy of the respective site, which can be either more conservation or usage-oriented. The present study was conducted in the Berchtesgaden National Park (southern Germany), as a highly protected area. The major challenge in detecting infested trees timely is

[1] National Park Administration Berchtesgaden, Department of Research and Monitoring, Doktorberg 6, D-83471 Berchtesgaden, E-Mail: lisa.mandl@npv-bgd.bayern.de
[2] University of Salzburg, Department of Geoinformatics, Schillerstrasse 30, A-5020 Salzburg, E-Mail: lisa-maria.mandl@stud.sbg.ac.at, stefan.lang@plus.ac.at

 DOI: 10.24407/KXP:1796049840

the fact that they appear physiologically green and do not show symptoms clearly observable by the human eye (ABDULLAH et al. 2019a). Nevertheless, biochemical changes during the initial phase of bark beetle infestation become visible due to the interaction between electromagnetic (EM) radiation of the sun and the leaves of the trees. Thus, certain portions in the EM spectrum can be used as stress indicators (HENDRY et al. 1987).

2 Material and Methods

2.1 Data

Input satellite data are Copernicus Sentinel-2 level 2A and level 3 data. We used best-available pixel composites between March and October only where illumination conditions for mono-temporal imagery were unfavourable. The 13 channels of Sentinel-2 are optimized for land surface observations and the high resolution of up to 10 m and the swath width of 290 km are ideal for detecting changes in vegetation. The revisiting time of these satellites is about five days (ESA 2017). In total, ten Sentinel-2 scenes from March to October 2020 were used (for concrete dates of data acquisition, Fig. 3). When atmospheric conditions permitted, two images per month were acquired. As reference data, we used aerial imagery from the management zone with a spatial resolution of 0.2 m from 2020. Grey-attack stages were derived by a supervised machine learning approach using a Random Forest ensemble model in R's machine learning package *SuperML*. The resulting dataset – the grey-attack detection – shows the state at the end of 2020. This means that sometime between April and August, the early stage of bark beetle infestation must occur on these plots, as this is the period when climatically optimal conditions for an outbreak are prevalent. Exactly this knowledge is essential if certain indicators are to be derived later. The plots classified as grey-attack are referred to as "test plots" from here on. Besides that, ground truth data was included. Search teams walk the same spots in the management zone every four weeks and enter bark beetle detections into this app. Field workers identify early-infested trees by opposite slope observation, paying particular attention to minimal changes in the colour of the spruce trees. Once such a tree is identified, an in-situ sighting is carried out, looking for possible dry dust and holes in the bark. These are ground-based signs of early infestation. Once early-infested plots are recorded with the app, data can be exported as a table and visualized in a GIS. Here, we used this information to assess the temporal accuracy of the developed method.

2.2 Software

The indices-based computations and the feature engineering were both conducted using the statistical software R (version 3.6.2) and the packages *sen2r* and *SuperML*, which provides a fit to Python's "scikit learn" package (R CORE TEAM 2021; RANGHETTI et al. 2020). Besides that, we applied a knowledge-based approach using the software SIAM™. This software – as opposed to the indices – considers the entire feature space of an image and divides it into so-called spectral-based semi-concepts (pre-classes). SIAM™ (release 88v7) stands for **S**atellite **I**mage **A**utomatic **M**apper and executes a preliminary, spectral rule-based classification, which is a discrete finite set of mutually exclusive and totally exhaustive spectral-based semi-concepts also referred to as spectral categories. It considers the bands Blue, Green, Red, NIR, SWIR-1 and SWIR-2. The benefit of SIAM™ for the purpose of this study is the capability to categorize satellite data into 96 spectral-based semi-concepts (BARALDI 2011). In this way, even minor changes in the "greenness" of vegetation can be detected and computed together with the changes in biophysical properties, represented by indices. These semi-concepts convert the continuous sub-symbolic variable "reflectance" into a given set of discrete categorical variables, whereas this process has to be reversible (BARALDI & BOSCHETTI 2012). However, these classes do not claim absolute uniqueness; several semantic categories may be valid options derived from one and the same pixel colour, like water or shadow.

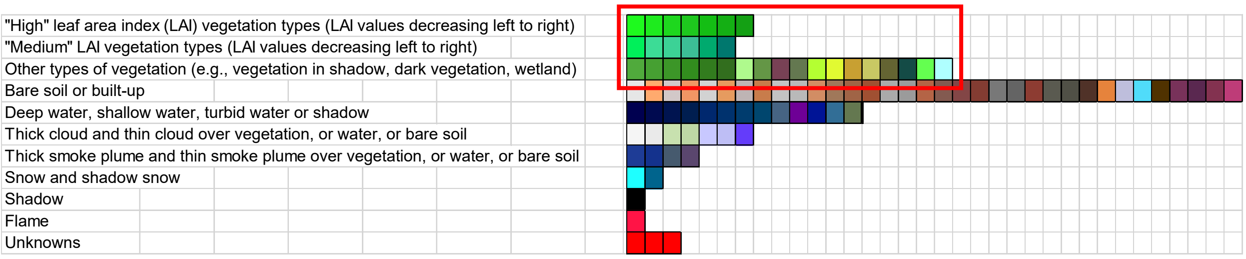

Fig. 1: Spectral-based semi concepts of the SIAM output (most important ones for this study in the red box), source: BARALDI et al. (2006)

As input, SIAM™ expects at least top-of-atmosphere (ToA) corrected data, meaning satellite data that is radiometrically calibrated into ToA (BARALDI 2011). For Sentinel-2 Level 2A data exhibiting bottom-of-atmosphere (BoA, also referred to as "SURF") correction, this requirement is given. In order to execute the SIAM™ software, Sentinel-2 Level 2A data were pre-processed including spatial resampling, image stacking and conversion to 8-bit ENVI format, the creation of an artificial thermal band as well as a noData mask. Finally, a SIAM batch file was created to calculate the spectral categories of the input data in batch mode.

2.3 Study Design

The core of this knowledge-based approach is a feature space partitioning, temporal response patterns and SVI's in combination with semantically enriched Sentinel-2 data (SIAM spectral categories). As a-priori knowledge is needed for first parametrization, the analyses were performed retrospectively for the year 2020. Grey attack test plots show where at the end of 2020 trees are attacked by bark beetles but there is no information available when infestation took place. Nevertheless, the grey-attack dataset is essential for further analysis. The two main processes during initial bark beetle infestation – subtle changes in the green tone of spruces and changes in the biochemical properties of trees – are represented by changes in the SIAM spectral categories and changes in pre-selected SVI's respectively. Both changes were solely observed within the grey-attack test plots because there is assured knowledge, that these areas must be attacked within the course of the year (Fig. 2). Within the test plots, inter-annual trajectories of pixels were observed. Besides the SIAM-based change detection, we developed a comprehensive set of six SVI's by applying a Principal Component Analysis (PCA) on 23 potentially suitable water stress and chlorophyll-related indices found in a literature research. Selected SVI's are shown in Fig. 5. As opposed to other methods, we defined index-specific thresholds based on statistical measurements. For this, we started three model runs using a set of descriptive statistics (min, max, quartiles and IQR) as potential thresholds. For each model run, the SVI change detection output was reclassified according to the thresholds. We found the minimum value serves best as lower threshold, while the 3rd quartile led to the best results for the upper threshold. The two basic assumptions are that (1) changes occuring in the SIAM spectral categories indicate bark beetle infestation at an early stage. This means that SIAM change detection values act as predictors and all changes in SIAM spectral categories within the test plots are considered as potentially early infestation pixels. (2) the interplay with SVI's concretise these first hints from the SIAM change detection by determining whether changes occur due to bark beetle infestation or due to other factors such as phenology, poor illumination, pixel shift or non-stationary surface type properties. In order to address only the host trees of bark beetles, the norway spruce tree (picea abies) is masked out by grouping SIAM spectral categories. This compensates for a missing data set for tree identification at the species level. At the end, conditional statements classify a raster cell as *early-infested*, applying following decision rule:

$$\textbf{Early infested} = \begin{cases} 1, \text{ if SIAM predictor} \parallel \text{SIAM coniferous} \parallel \text{index A} \parallel \text{index B} \parallel \\ \text{index C} \parallel \ldots = 1, 0 \text{ otherwise} \end{cases}$$

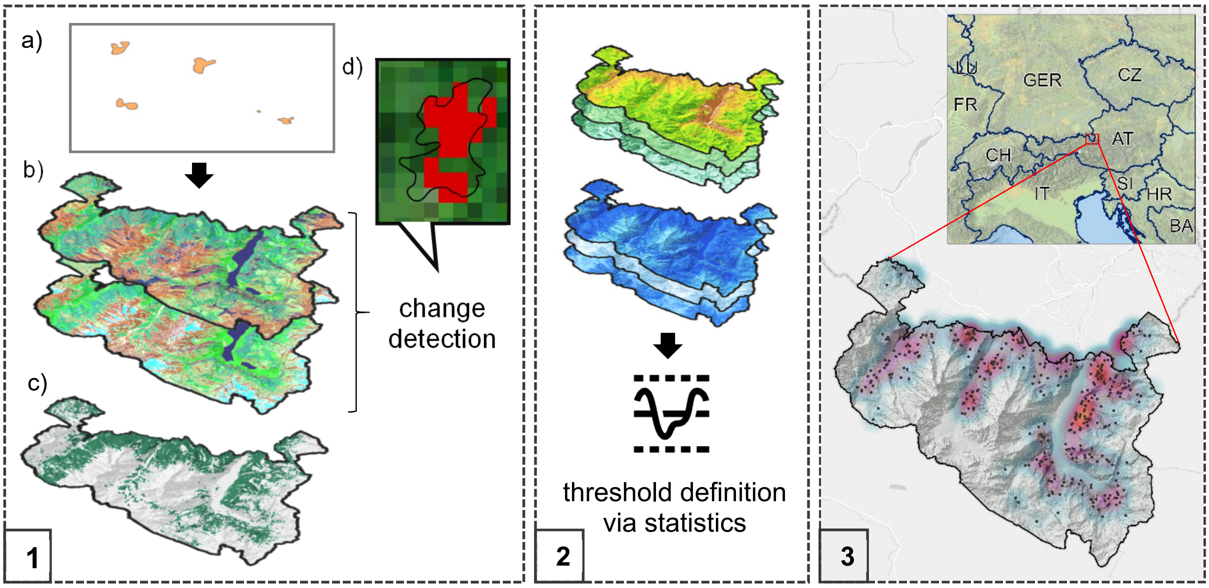

Fig. 2: Panel 1: SIAM-based analysis; a) Test plots within change detection is carried out, b) SIAM change detection, here for two time stamps, c) coniferous mask d) reclassified SIAM predictor values within test plot (black outline). Panel 2: Indices-based analysis: Change detection of chlorophyll-related indices (greenish) and water stress-related indices (blueish), based on which the thresholds are derived. Panel 3: Location of the study site and final infestation map, here for the entire year

All cells classified as *early-infested* are double-checked in order to minimize the potential error that may result from pixel shift or adverse illumination conditions. Then, in the second iteration, it is not only checked for which cells conditional statements are true, but also whether a particular cell has been classified as *early-infested* in the previous time step. If this hold true, the cell is considered infested; otherwise, it is reset to *healthy*. Finally, the impact of the six selected SVI's was analysed by computing feature importance based on random forest (RF).

3 Results

3.1 Spectral separability and temporal variation of canopy reflectance under bark beetle infestation

In total, 350 randomly selected pixels for each of the classes *healthy, early-infested* and *grey-attack* were included into the analysis; their spectral reflectance (median) was plotted together with the error bands.

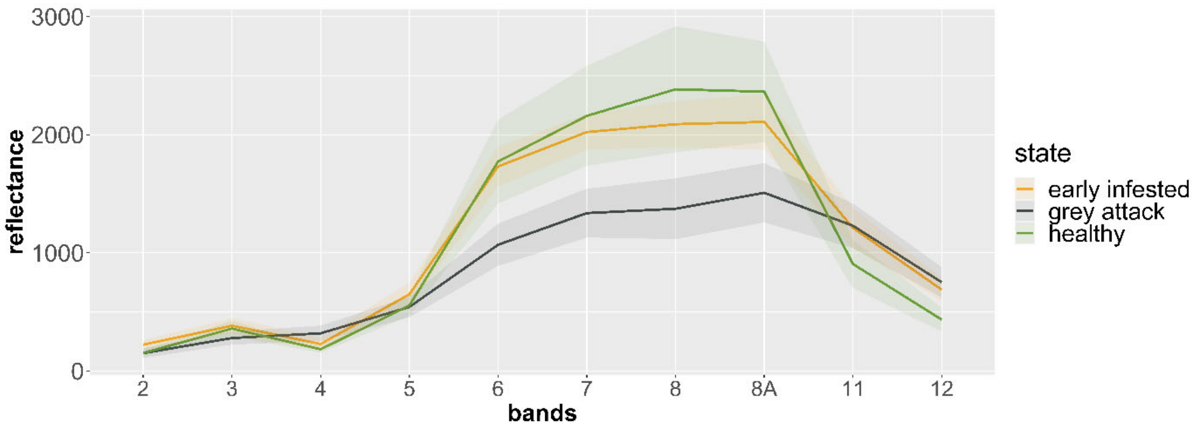

Fig. 3: Spectral behaviour of green-attack-, grey-attack and healthy pixels in the electromagnetic spectrum

Fig. 3 shows that healthy pixels differ significantly from grey-attack pixels in terms of their spectral behaviour. Especially in the red-edge bands and in the NIR and SWIR part of the EM spectrum (bands 5 to 12) the differences are clearly visible. The signal is much weaker in the VIS range. When comparing healthy pixels with the pixels classified as early-infested, there are significantly smaller differences, both in the VIS as well as in the red-edge, NIR and SWIR range. The greatest distinguishability between the two stages is seen at band 8 and 8A, where early-infested pixels have lower reflectance values and at bands 11 and 12, i.e. in the NIR-1, NIR-2 and SWIR range, where reflectance is higher compared to healthy pixels. By analysing single time stamps, inter-annual differences can be observed. Particularly big differences of reflectance per time stamp emerge for bands 8, 8A, 11 and 12 (Fig. 4).

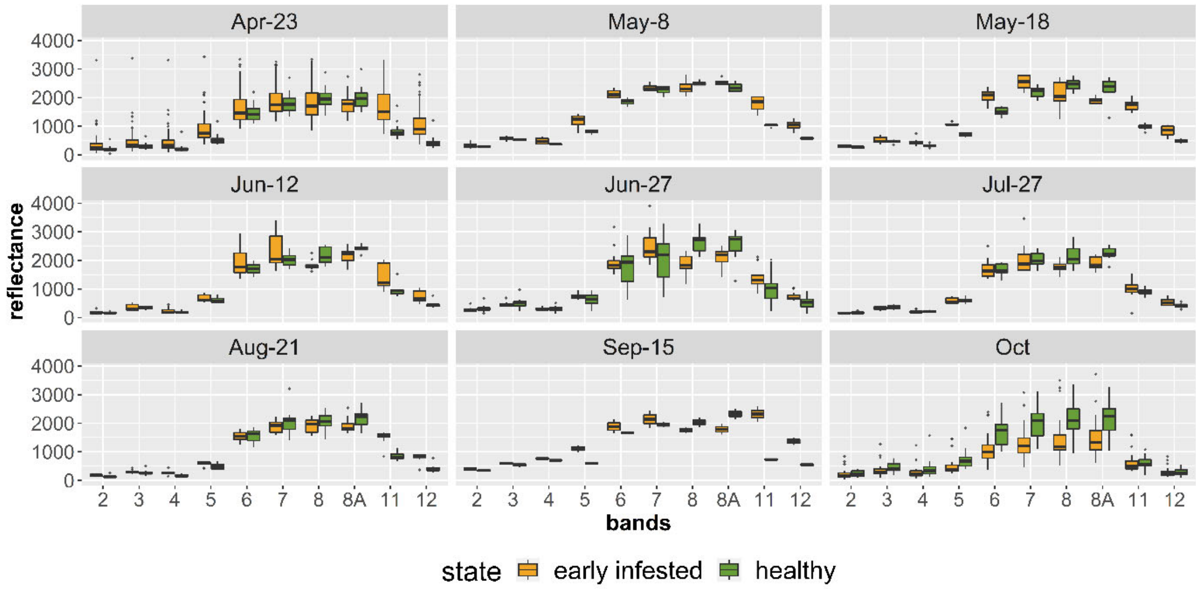

Fig. 4: Reflectance for healthy and early-infested pixels per band and time step. There is stronger scatter for healthy pixels, whereas the signal appears clearer for early-infested pixels

In these wavelength ranges, the reflectance for pixels classified as *early-infested* differs significantly from the class *healthy* as also shown by a t-test (see Tab. 1).

Tab. 1: Significance levels for the bands 8 (NIR-1), 8A (NIR-2), 11 (SWIR-1) and 12 (SWIR-2). p-values are computed by applying a student-t-test

Date	***p*-value B8**	***p*-value B8A**	***p*-value B11**	***p*-value B12**
2020-05-08	0.211	0.102	**< 0.001**	**< 0.001**
2020-05-18	0.101	0.034	**< 0.001**	**0.002**
2020-06-12	**0.020**	**0.026**	**0.013**	**0.004**
2020-06-27	**< 0.001**	**0.003**	0.065	**0.002**
2020-07-27	**0.005**	**0.001**	0.205	**0.004**
2020-08-21	0.195	**0.020**	**< 0.001**	**< 0.001**
2020-09-15	0.306	0.172	**< 0.001**	**< 0.001**
2020-10	**0.003**	**0.004**	0.667	0.938

* in bold values with p < 0.05

Tab. 1 shows significance levels for bands 8, 8A, 11 and 12. Especially for bands 8A, 11 and 12 – NIR-2, SWIR 1 and SWIR 2 – the *p*-value mostly is below the significance threshold of 0.05. That means the null hypothesis – there are no significant differences between healthy and early-infested pixels – should be rejected. For NIR-1 (band 8), differences seem to be less clear as it is the case for the NIR-2 and SWIR region. Only four time steps fall below the significance threshold of 0.05 and can be considered *significantly* different. The remaining *p*-values > 0.05 give evidence that differences between healthy and early-infested pixels are not significant. This is particularly true for band 8 and reflects the findings in ADAMCZYK AND OSBERGER (2015) who claim that the NIR range is particularly useful for detecting advanced stages of bark beetle infestation but not that much for early stage detection.

3.2 Impact of indices on classification result based on impurity-based feature importance

The results of the impurity-based feature importance (Gini-importance) for the whole year shows that DSWI is the most relevant index for the model output. It is followed by NDI45 and NDWI. The impact of TCW and especially NDRE3 and NGRDI is relatively low (Fig. 5a).

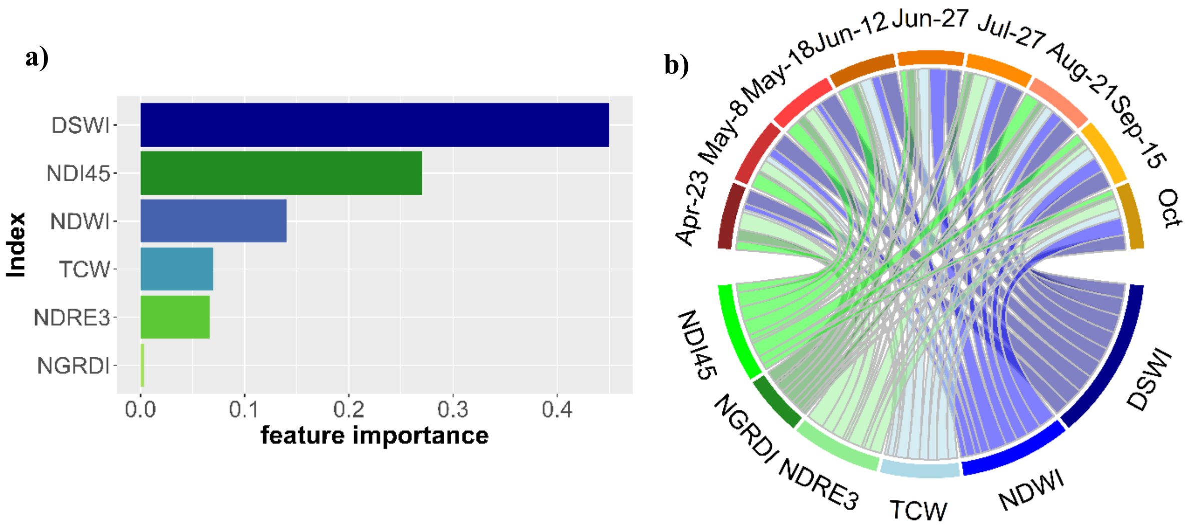

Fig. 5: a) Feature importance computed for the whole year. b) Relationship between the single time steps satellite data was acquired (top), the according indices (bottom) and the feature ranking (indicated by the thickness of the connecting lines)

When comparing predictor importance for the single time steps (Fig. 5b and 6), it can be observed that the order of indices is swapping. The chord chart (Fig. 5b) shows the interrelation between the time stamps of the satellite data, the SVI's and feature importance of SVI's. Thicker lines indicate a higher ranking of the corresponding index depending on the date. It is striking that for the months April to May the pigment- and chlorophyll-related indices (in green) dominate the top ranking positions, while from June onwards the water stress-related indices (in blue) get more important. This is also shown in Fig. 6.

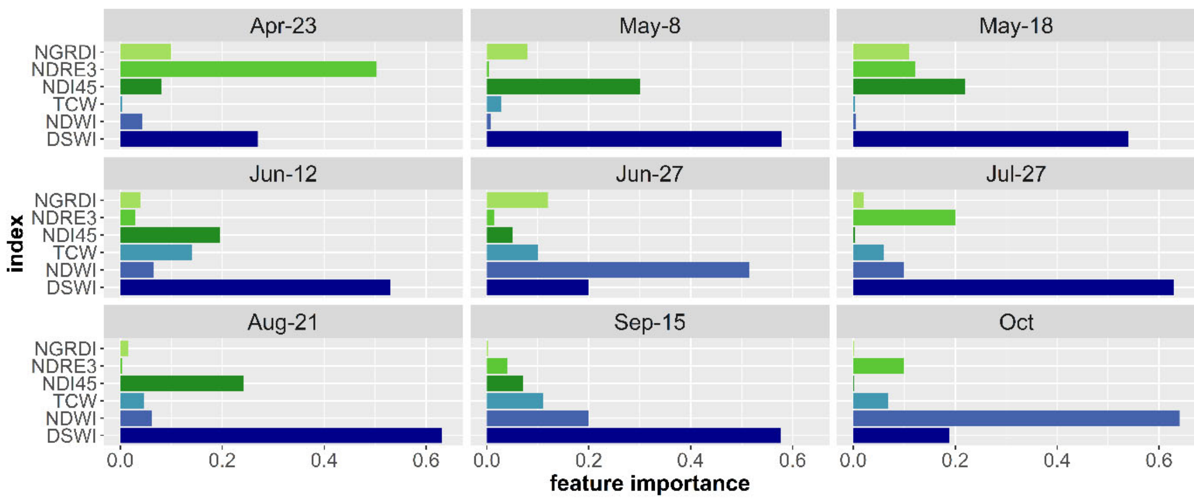

Fig. 6: Feature importance computed for single time steps. Inter-annual differences in the feature ranking is observable

Tab. 2: Accuracy of the RF model for determining feature importance

Time step	Accuracy	OOB error
April 23rd	36.22%	0.673
May 8th	54.667%	0.231
May 18th	72.00%	0.158
June 12th	62.50%	0.273
June 27th	81.667	0.108
July 27th	66.667%	0.237
August 21st	70.588%	0.143
September 15th	78.286%	0.114
October	37.99%	0.683

The seasonal dependence of SVI's on predictor importance is a key finding and should be considered in follow-up studies. The predictive performance of the RF feature importance model for the whole year is 61.8%. This value seems to be relatively low, but can be explained when evaluating feature importance and accuracy for each single time stamp, which is just like out-of-bag (OOB) error, quite variable as shown in Tab. 2. In summary, intra-annual differences in predictor importance and accuracy as well as out-of-bag (OOB) error are noticeable. The rather low accuracy of the model for April and October can be attributed to the poorer illumination conditions of the satellite data in these months.

3.3 Validation

Both spatial and temporal dimensions were considered in the validation process using the grey-attack dataset and ground truth data as reference data (cf. chapter 2.1). Notably, the data situation is not good enough for an all-encompassing and fully representative accuracy assessment. Reference data is only available for the so-called management zone of the Berchtesgaden National Park, which accounts for less than one third of the entire area (~ 6,300 ha). Nevertheless, based on available data, we will evaluate the spatial and temporal performance of the method.

From a spatial perspective, the method we developed in this study detects early bark beetle patches with an accuracy of 76% compared to the grey-attack reference dataset. For better comparability, we rasterized the polygons of the grey-attack dataset and assessed for both, on pixel and on plot level, where plots refer to a group of more than four individual trees. That means that all single trees classified as early-infested were excluded for plot level accuracy assessment. We found out two main error sources: (1) the method generally includes too many pixels that should not be considered early-infested according to the reference data (error of commission); (2) *single* infested trees cannot be detected but only patches – meaning an accumulation of trees. Reasons leading to these sources of error are discussed in the following chapter.

From a temporal perspective, earlier respectively later detection scatters from three weeks earlier until three weeks later as compared to ground truth data. The results of the temporal accuracy assessment show that there are no trends in temporal accuracy between months. Thus, bark beetle infestation is not recorded particularly early or late in any of the time steps. Accordingly, the temporal differences are most likely due to data availability, but not due to data quality. Overall, the temporal agreement between the reference data and the modelled results is good. A high proportion of the predicted values indicate bark beetle infestations prior to the findings in the field. The maximum deviation in negative direction, i.e. temporally after the detection in the field, is three weeks. Undoubtedly, there is a high dependency between accuracy and data availability such that the timing of data acquisition is a major driver when it comes to an early detection.

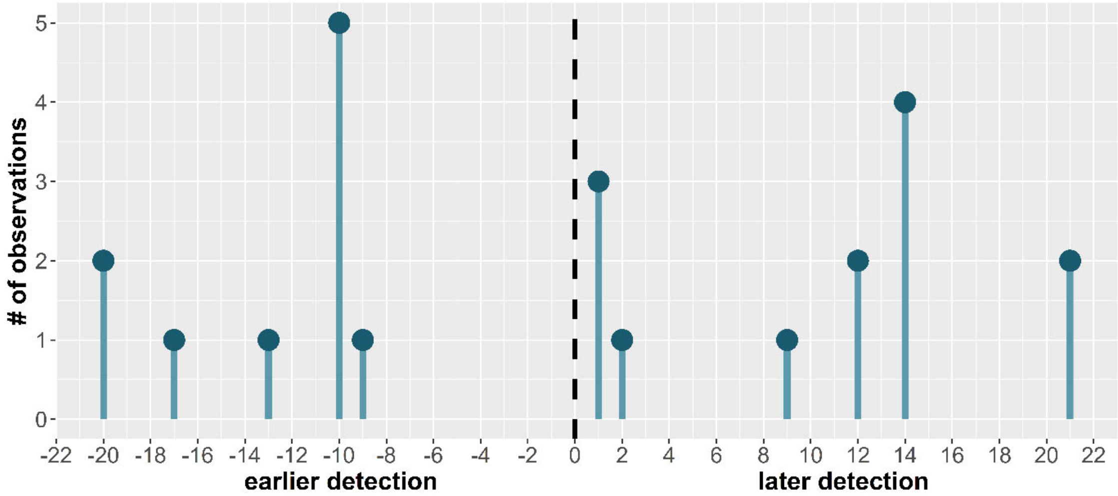

Fig. 7: Graphical representation of the temporal accuracy. The dashed line indicates the date of ground truth recording. All entries left from '0' mean earlier detection compared to ground truth data, all entries right mean later detection

4 Discussion

4.1 Methodological perspective

The method presented in this study is able to detect early stages of bark beetle infestation with the help of the lightweight software SIAM™ and the use of spectral vegetation indices. Both calculations can be realised within a very short timeframe, as an important feature when it comes to the operational use of this approach. Compared to field sights, the presented method detects bark beetle attacks up to three weeks earlier or later than the field workers do. The fairly wide range may be attributed to data availability. It is challenging to determine whether the method is really capable to detect green-attack stages. The whole workflow is based on alterations in SIAM spectral categories. Undoubtedly, the software can only indicate changes when changes already occur in the spectral range. Therefore, the term green-attack may be misleading here, which is why we use the term early detection in this study. On the other hand, the field sightings are also based on minimal spectral changes, which is why green-attack is not quite correct there either, but commonly used in fact. In summary, the term green-attack is a matter of definition and even in literature not always consistent. Moreover, bark beetle attacks are a continuous process, meaning that various environmental factors drive this particular forest ecosystem dynamic in time and space (BÁRTA et al. 2021). Furthermore, indices used as proxies, always need to be viewed critically, regardless of whether they are multi-dimensional indices such as the Tasseled Cap Components or unidimensional indices. This "lack of confidence" is attributable to the difficult understanding and interpretation of them. Of course, they give hints to facts like a decrease in the water availability. However, they also reflect atmospheric and landscape variations that are extremely difficult to impossible to filter out or to map them to fixed points on the index scale (MOFFIET et al. 2006). The information content of spectral vegetation indices is therefore limited. On the other hand, the use of indices has already proven its great potential in a variety of applications. Thus, they definitely have their right to exist in remote sensing, but at the same time, their limitations must be known and taken into account.

4.2 Resolution, data quality and data availability

Concerning the effect of data resolution, there will always be mixed pixels at a spatial resolution of 10 m. Detection methods – no matter if early detection or grey-attack detection may come to its limit when there are pixels that do not purely represent spruce stands (MEDDENS et al. 2013). An evaluation of spectral mixture effects would require very high resolution (VHR) data, i.e. UAV data or the application of a radiative transfer model like the DART model, which can be used for sensitivity analysis of forest reflectance (BÁRTA et al. 2021). Generally speaking, high spatial resolution is necessary when bark beetle infestations occur at endemic levels, as the infested areas are usually isolated patches. In contrast, the relevance of spatial resolution decreases when the infestation is epidemic, since the infested areas are then mostly large, contiguous patches (FERNANDEZ-CARRILLO et al. 2020; KAUTZ et al. 2011). In addition, radiometric resolution is a potential source of error, as it affects the actual information content, and the ability to differentiate between slight differences in EM reflectance. This is especially important for this application purpose. It could be argued in this context that a better result could have been achieved if the input for SIAM™ did not have to be scaled down to 8 bit. However, since 8-bit data is a practical constraint for using SIAM™, such an assumption cannot be verified. Finally, it must also be remembered that high radiometric resolution alone is not sufficient to detect early-infested bark beetle trees. ABDULLAH et al. (2019b) proved that in a comparison of Sentinel-2 and Landsat data.

4.3 Accuracy

The high error of commission (39%) in the spatial accuracy assessment can primarily explained by the relatively early image flight campaign (early September), to which the grey-attack machine learning approach is applied and from which the grey-attack reference dataset results. Especially from July onwards, the accuracy assessment is subject to uncertainties, as it is highly likely that trees will not have discoloured when reference data was acquired and thus will not be detected by the grey-attack algorithm, even if these trees are infested. All pixels classified as *early-infested* from July and later, but not appearing in the grey-attack dataset, would thus require re-analysis with data from subsequent years. When evaluating the temporal accuracy, it should be mentioned that field recording of early infestation is not "obvious", meaning that even in the field the error is relatively high. Thus, the absence of reference data on a spot classified as *early-infested* does not necessarily indicate an error of omission, but may equally be due to difficulty in locating infested spruce trees, especially in a challenging terrain such as in the Berchtesgaden National Park. Finally, accuracy may be improved by the availability of data that classifies forest stands at the species level. At the moment, our approach is applied to all coniferous stands, no matter if there is Norway spruce or any other coniferous tree present.

5 Conclusion and Outlook

Our proposed method provides a novel prototypical tool to detect forest stress from bark beetles by considering space, time and spectral characteristics of remotely sensed data. The method can be considered a form of "hybrid AI", i.e. combining a deductive, learning-from-rules approach with an inductive, learning-from-samples method. The distinctive feature of the method is the use of semantically enriched Sentinel-2 data via the highly advanced, knowledge-based software SIAM™ and the derivation of predictor values, which contributed significantly to the success of this study. Unlike the use of SVI's alone, spectral categories of SIAM™ include the complete feature space, so that no – possibly relevant – information is lost. This unique research design outperforms conventional methods of early bark beetle detection, both in terms of the time aspect of fieldwork and the accuracy of other remote sensing approaches. Further advantages of using SIAM™ is the complete automation of the software, which does not require any parameters from users or samples. The high level of automation also contributes to the robustness to changes in input data. In addition to Sentinel-2 data, all other at least top-of-atmosphere corrected optical satellite can be used as input, including VHR data exhibiting infrared bands. Thus, the workflow can also be adapted for other scale levels. A shortcoming of this method is that single trees cannot be detected due to the resolution of Sentinel-2 data. In addition, at least two satellite scenes per month are required to monitor the early stages of bark beetle infestation reliably. Otherwise, temporal accuracy decreases significantly. Results from this approach proved that especially water-stress related indices as well as the vegetation red-edge and the SWIR ranges of the EM spectrum show high sensitivity for early bark beetle detection. Future development shall focus on building up a samples database in order to apply more sophisticated and self-adaptive deep learning algorithms, which are currently state-of-the-art in recognition performance. This allows also to run the tool in real-time, i.e. without a-priori data (here the grey-attack dataset). Alternatively, this approach can be repeated for several years to derive more robust index-specific thresholds, thus staying with a purely index-based method. Regardless of the choice of the methodology, a monitoring system that detects bark beetle infestations at an early stage makes an important contribution both to the prevention of large-scale tree mortality and to ecological research. The interaction of modern, satellite-based technologies and the on-site knowledge of forest experts proves to be very beneficial and shows that ecological field research and remote sensing-based monitoring complement each other very well and profitably.

6 References

ABDULLAH, H., SKIDMORE, A., DARVISHZADEH, R. & HEURICH, M., 2019a: Timing of red-edge and shortwave infrared reflectance critical for early stress detection induced by bark beetle (Ips typographus, L.) attack. International Journal of Applied Earth Observation and Geoinformation, **82**, 101900.

ABDULLAH, H., SKIDMORE, A. K., DARVISHZADEH, R. & HEURICH, M., 2019b: Sentinel-2 accurately maps green-attack stage of European spruce bark beetle (Ips typographus, L.) compared with Landsat-8. Remote Sensing in Ecology and Conservation, **5**(1), 87-106. https://doi.org/10.1002/rse2.93. https://doi.org/10.1002/rse2.93.

ADAMCZYK, J. & OSBERGER, A., 2015: Red-edge vegetation indices for detecting and assessing disturbances in Norway spruce dominated mountain forests. International Journal of Applied Earth Observation and Geoinformation, **37**.

BARALDI, A., 2011: Satellite Image Automatic Mapper™ (SIAM™) - A Turnkey Software Executable for Automatic Near Real-Time Multi-Sensor Multi-Resolution Spectral Rule-Based Preliminary Classification of Spaceborne Multi- Spectral Images. Recent Patents on Space Technology, **1**, 81-106.

BARALDI, A. & BOSCHETTI, L., 2012: Operational Automatic Remote Sensing Image Understanding Systems: Beyond Geographic Object-Based and Object-Oriented Image Analysis (GEOBIA/GEOOIA). Part 1: Introduction. Remote Sensing, **4**(9), 2694-2735. https://www.mdpi.com/2072-4292/4/9/2694.

BARALDI, A., PUZZOLO, V., BLONDA, P., BRUZZONE, L. & TARANTINO, C., 2006: Automatic Spectral Rule-Based Preliminary Mapping of Calibrated Landsat TM and ETM+ Images. Geoscience and Remote Sensing, IEEE Transactions on, **44**, 2563-2586.

BÁRTA, V., LUKEŠ, P. & HOMOLOVÁ, L., 2021: Early detection of bark beetle infestation in Norway spruce forests of Central Europe using Sentinel-2. International Journal of Applied Earth Observation and Geoinformation, **100**, 102335. https://www.sciencedirect.com/science/article/pii/S0303243421000428.

DELEGIDO, J., VERRELST, J., ALONSO, L. & MORENO, J., 2011: Evaluation of Sentinel-2 Red-Edge Bands for Empirical Estimation of Green LAI and Chlorophyll Content. Sensors, **11**(7).

ESA. 2017: Sentinel-2: Color vision for Copernicus.

FER, I., GARDELLA, A. K., SHIKLOMANOV, A. N., CAMPBELL, E. E., COWDERY, E. M., DE KAUWE, M. G., DESAI, A., DUVENECK, M. J., FISHER, J. B., HAYNES, K. D., HOFFMAN, F. M., JOHNSTON, M. R., KOOPER, R., LEBAUER, D. S., MANTOOTH, J., PARTON, W. J., POULTER, B., QUAIFE, T., RAIHO, A., SCHAEFER, K., SERBIN, S. P., SIMKINS, J., WILCOX, K. R., VISKARI, T. & DIETZE, M. C., 2021: Beyond ecosystem modeling: A roadmap to community cyberinfrastructure for ecological data-model integration. Global Change Biology, **27**(1), 13-26.

FERNANDEZ-CARRILLO, A., PATOČKA, Z., DOBROVOLNÝ, L., FRANCO-NIETO, A. & REVILLA-ROMERO, B., 2020: Monitoring Bark Beetle Forest Damage in Central Europe. A Remote Sensing Approach Validated with Field Data. Remote Sensing, **12**(21).

GALVÃO, L. S., FORMAGGIO, A. R. & TISOT, D. A., 2005: Discrimination of sugarcane varieties in Southeastern Brazil with EO-1 Hyperion data. Remote Sensing of Environment, **94**(4), 523-534. http://www.sciencedirect.com/science/article/pii/S0034425704003669.

HARDISKY, M., KLEMAS, V. & SMART, A., 1983: The influence of soil salinity, growth form, and leaf moisture on the spectral radiance of Spartina Alterniflora canopies. Photogrammetric Engineering and Remote Sensing, **48**, 77-84.

HENDRY, G. A. F., HOUGHTON, J. D. & BROWN, S. B., 1987: The degradation of chlorophyll - A biological enigma. New Phytologist, **107**(2), 255-302.

HUNT, E., DAUGHTRY, C., EITEL, J. & LONG, D., 2011: Remote Sensing Leaf Chlorophyll Content Using a Visible Band Index. Agronomy Journal, **103**, 1090.

KAUTZ, M., DWORSCHAK, K., GRUPPE, A. & SCHOPF, R., 2011: Quantifying spatio-temporal dispersion of bark beetle infestations in epidemic and non-epidemic conditions. Forest Ecology and Management, **262**, 598-608.

MEDDENS, A. J. H., HICKE, J. A., VIERLING, L. A. & HUDAK, A. T., 2013: Evaluating methods to detect bark beetle-caused tree mortality using single-date and multi-date Landsat imagery. Remote Sensing of Environment, **132**, 49-58. https://www.sciencedirect.com/science/article/pii/S0034425713000060.

MOFFIET, T., MENGERSEN, K., KING, R., ARMSTON, J. & WITTE, C., 2006: Modelling of foliage projected cover using Landsat-7 spectral imagery: Spectral indices for greenness and brightness. 13th Australian Remote Sensing and Photogrammetry Conference, Canberra, Australia, 20-24.

R CORE TEAM, 2021. A Language and Environment for Statistical Computing. R Foundation for Statistical Computing. Retrieved from https://www.R-project.org/.

RANGHETTI, L., BOSCHETTI, M., NUTINI, F. & BUSETTO, L., 2020: sen2r: An R toolbox for automatically downloading and preprocessing Sentinel-2 satellite data. Computers & Geosciences, **139**. https://sen2r.ranghetti.info.

SENF, C., PFLUGMACHER, D., HOSTERT, P. & SEIDL, R., 2017: Using Landsat time series for characterizing forest disturbance dynamics in the coupled human and natural systems of Central Europe. ISPRS journal of photogrammetry and remote sensing : official publication of the International Society for Photogrammetry and Remote Sensing (ISPRS), **130**, 453-463. https://doi.org/10.1016/j.isprsjprs.2017.07.004.

SHI, Y., WANG, T., SKIDMORE, A. K. & HEURICH, M., 2020: Improving LiDAR-based tree species mapping in Central European mixed forests using multi-temporal digital aerial colour-infrared photographs. International Journal of Applied Earth Observation and Geoinformation, **84**. http://www.sciencedirect.com/science/article/pii/S0303243419300340.

SUDMANNS, M., TIEDE, D., LANG, S., BERGSTEDT, H., TROST, G., AUGUSTIN, H., BARALDI, A. & BLASCHKE, T., 2020: Big Earth data: disruptive changes in Earth observation data management and analysis? International Journal of Digital Earth, **13**(7), 832-850. https://doi.org/10.1080/17538947.2019.1585976.

THOM, D. & SEIDL, R., 2016: Natural disturbance impacts on ecosystem services and biodiversity in temperate and boreal forests: Disturbance impacts on biodiversity and services. Biological Reviews, **91**.